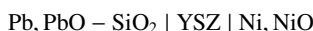


M. KOPYTO*, W. PRZYBYŁO*, B. ONDERKA**, K. FITZNER**

THERMODYNAMIC PROPERTIES OF $\text{Sb}_2\text{O}_3\text{-SiO}_2$ AND $\text{PbO-Sb}_2\text{O}_3\text{-SiO}_2$ LIQUID SOLUTIONS

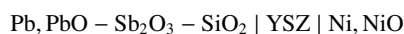
WŁAŚCIWOŚCI TERMODYNAMICZNE CIEKŁYCH ROZTWORÓW $\text{Sb}_2\text{O}_3\text{-SiO}_2$ I $\text{PbO-Sb}_2\text{O}_3\text{-SiO}_2$

Thermodynamic properties of the liquid PbO-SiO_2 and $\text{Sb}_2\text{O}_3\text{-SiO}_2$ solutions were derived from the results of the electrochemical studies by the use of solid oxide galvanic cells with YSZ electrolyte. Activities of PbO in silicate melts were determined directly in the temperature range from 850 to 1025 K and for SiO_2 mole fractions 0.2, 0.3, 0.4 and 0.5 from measured e.m.f.'s of the cell:



relatively to Gibbs energy change of pure PbO formation.

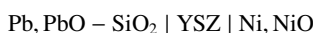
The thermodynamic properties of $\text{Sb}_2\text{O}_3\text{-SiO}_2$ liquid solutions were derived indirectly from the measurements conducted with the cell of the type:



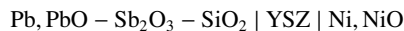
in ternary $\text{PbO-Sb}_2\text{O}_3\text{-SiO}_2$ liquid solutions in the temperature range from 1070 to 1280 K.

Two pseudobinary phase diagrams, namely, PbO-SiO_2 and $\text{PbO-Sb}_2\text{O}_3$ were optimized, and next using the obtained results the diagram of $\text{Sb}_2\text{O}_3\text{-SiO}_2$ system, and the liquidus in the pseudoternary $\text{PbO-Sb}_2\text{O}_3\text{-SiO}_2$ were predicted.

Na podstawie badań elektrochemicznych z wykorzystaniem ogniw galwanicznych ze stałym elektrolitem cyrkonowym YSZ określono właściwości termodynamiczne ciekłych roztworów PbO-SiO_2 i $\text{Sb}_2\text{O}_3\text{-SiO}_2$. W zakresie temperatury od 850 do 1025 K dla stężeń molowych SiO_2 0.2, 0.3, 0.4 i 0.5 wyznaczono aktywności PbO w żużlu krzemionkowym w odniesieniu do energii swobodnej Gibbsa tworzenia czystego PbO . Obliczenia wykonano bezpośrednio ze zmierzonych doświadczalnie sił elektromotorycznych ogniwa o schemacie:



Właściwości termodynamiczne ciekłych roztworów $\text{Sb}_2\text{O}_3\text{-SiO}_2$ określono pośrednio z danych termodynamicznych otrzymanych z pomiarów dla ciekłych roztworów $\text{PbO-Sb}_2\text{O}_3\text{-SiO}_2$. Zastosowane tu ogniwa typu:



pracowały w zakresie temperatury 1070-1280 K.

Zoptymalizowano dane termodynamiczne dla dwóch pseudopodwójnych układów fazowych PbO-SiO_2 and $\text{PbO-Sb}_2\text{O}_3$ i wyznaczono ich diagram fazowe. Tak wyznaczone dane termodynamiczne zastosowano do oszacowania wykresu fazowego $\text{Sb}_2\text{O}_3\text{-SiO}_2$ i określenia przewidywanego kształtu powierzchni likwidus w pseudopotrójnym układzie tlenkowym $\text{PbO-Sb}_2\text{O}_3\text{-SiO}_2$.

1. Introduction

Silver production from anodic sledges which are left after electrorefining of copper is based on the so called Kaldo process, in which two subsequent stages of reduc-

tion and oxidation take place. After the second step, solutes from silver are transferred into the slag phase. In order to predict the distribution behavior of the impurities between metal (which is silver with traces of bismuth, lead and antimony as the most common) and the slag un-

* INSTITUTE OF METALLURGY AND MATERIALS SCIENCE, POLISH ACADEMY OF SCIENCES, 30-059 KRAKOW, 25 REYMONTA STR., POLAND

** AGH UNIVERSITY OF SCIENCE AND TECHNOLOGY, FACULTY OF NON-FERROUS METALS, LABORATORY OF PHYSICAL CHEMISTRY AND ELECTROCHEMISTRY, 30-059 KRAKOW, 30 MICKIEWICZA AVE., POLAND

der fixed temperature and partial oxygen pressure, thermodynamic properties of both liquid solutions, namely, metallic phase and the slag phase must be known. Thus, thermodynamic properties of at least four component oxides solution: $\text{SiO}_2 + \text{Bi}_2\text{O}_3 + \text{Sb}_2\text{O}_3 + \text{PbO}$ should be known. The inspection of literature on this subject indicates that no such information exists. Indeed, this system is not easy to work with, due to a high melting point of SiO_2 on the one hand, and the high vapour pressure of the rest of the oxides on the other. It seems that the only chance to work out a sensible solution to this problem is to gather experimental information on all binary systems which contribute to this particular quaternary solution (six of them altogether), and then add them up according to a certain thermodynamic model in order to predict behavior of this multicomponent oxide solution.

A thorough literature search showed that phase diagram of only $\text{PbO} + \text{SiO}_2$ binary system is well known [1]. Despite high melting temperature of one of the constituent oxides it is characterized by a wide range of liquid solutions – up to $X_{\text{SiO}_2} = 0.7$ at 1273 K. In the solid state silicates of $n\text{PbO} \cdot m\text{SiO}_2$ type appear, and two of them, PbSiO_3 and Pb_2SiO_4 melt congruently, at 1037 and 1016 K, respectively. First activity measurements in $\text{PbO} - \text{SiO}_2$ liquid solutions were carried out by Callow [2], Richardson and Webb [3] and Minenko and Ivanova [4]. Application of solid electrolytes on ZrO_2 basis in galvanic cells stimulated more activity studies of PbO in this liquid solution. For example, works of Sridhar and Jeffes [5], Kozuka and Samis [6], Charette and Flenegas [7], and Kapoor and Frohberg [8] provided a lot of thermodynamic data of the liquid oxide phase. Also, partial enthalpies of mixing of PbO and SiO_2 in liquid solution were obtained by Østvold and Kleppa [9] who used self-made drop calorimeter.

The other two systems: $\text{PbO} + \text{Bi}_2\text{O}_3$ and $\text{PbO} + \text{Sb}_2\text{O}_3$ are not so well known. Phase diagram of the $\text{PbO} + \text{Bi}_2\text{O}_3$ system was studied by Boivin and Tridot [10] as well as Biefeld and White [11]. The single study of Mehrotra, Frohberg and Kapoor [12] provides activity data for both components at 1173 K. These data have not been verified so far.

The $\text{PbO} - \text{Sb}_2\text{O}_3$ phase diagram is even less known. It was given first time by Maier and Hincke [13] in 1932. Barthel [14] and Pelzel [15] determined the liquidus in PbO -rich part of this system which agreed closely with Maier and Hincke's data [13]. This study was later repeated and Zunkel and Larson [16] by DTA analysis and metal-slag equilibration. Determination of the entire liquidus by Hennig and Kohlmayer [17] showed remarkable disagreement with the data mentioned above. It seems that only Sb_2O_3 -rich part of the diagram can-

not be questioned. However, once the composition of PbSb_2O_4 phase is reached and liquidus temperature rises, there are some doubts if PbO -rich part of this phase diagram can be trusted. None of the investigators mentioned above reported any mutual solubility in the $\text{PbO} - \text{Sb}_2\text{O}_3$ solid system. The existence of (PbO) terminal solution suggested by the only result of metal-slag equilibration done by Zunkel and Larson [16] is not certain and has not been taken into consideration in our work.

The activity of Sb_2O_3 in the liquid solution was measured by Sugimoto *et al.* [18] and recently by Itoh *et al.* [19]. They both used electrochemical method employing galvanic cells with solid electrolyte. The results of both studies showed negative deviation from the Raoult's Law, which is compatible with the existence of the PbSb_2O_4 solid phase in this system. Maier and Hincke [13] are the only investigators who made vapour-pressure measurements on liquid slags in the temperature range of interest but their data gave only one point in the desirable composition range. Their Sb_2O_3 activity result obtained at 973 K agree reasonably well with the results of McClincy and Larson [20], who used gas saturation method.

There are three different studies which suggest the phase equilibria in the $\text{Bi}_2\text{O}_3 + \text{Sb}_2\text{O}_3$ system: Tairi *et al.* [21], Turkoglu *et al.* [22] and Jingkui *et al.* [23]. All these studies agree at one point: there exists, one to one BiSbO_3 solid phase with a high melting point, which divides the system into two parts. Bi_2O_3 -rich part shows numerous phases with solid solutions between them. Equilibrium with the liquid phase is not known in this part of the system. According to Jingkui *et al.* [23] Sb_2O_3 -rich part looks like the eutectic system. To a certain extent it is similar to the system suggested by Tshernogorenko *et al.* [24] who studied reciprocal reactions in the $\text{Sb} - \text{Bi} - \text{O}$ system. Two other studies [21] and [22] did not show the course of the liquidus line in this range of concentrations. Instead, the existence of the solid solutions is suggested. Recently, new information about thermodynamic properties of these liquid solutions was given by Krzyżak and Fitzner [25].

The $\text{Bi}_2\text{O}_3 + \text{SiO}_2$ system, another binary constituent of the four component $\text{SiO}_2 + \text{Bi}_2\text{O}_3 + \text{Sb}_2\text{O}_3 + \text{PbO}$ solution has been recently reviewed in the work of Kopyto *et al.* [26]. Finally, no thermodynamic and phase diagram data are known to exist for $\text{Sb}_2\text{O}_3 + \text{SiO}_2$ system.

This short literature survey indicates that it is not possible at present to predict properties of the quaternary slag solution. In order to gather more data on respective binary systems, attempts have been made in this study to determine the thermodynamic properties of the liquid phase in $\text{Sb}_2\text{O}_3 - \text{SiO}_2$ system. In order to check the reliability of galvanic cell performance, activity de-

termination and the thermodynamic properties of liquid PbO-SiO₂ phase were studied first.

2. Experimental

Materials

Pure antimony (99.9%), was obtained from Fluka AG (Switzerland). Lead was delivered by ZMR Skawina (Poland) and it was 99.99% pure. The lead oxide and antimony sesquioxide of 99.9% purity were obtained from Fluka AG and from International Enzymes Ltd. (UK), respectively. SiO₂ powder was obtained from silica glass, after grinding and boiling in nitro-hydrochloric acid. Dried in the next step and then annealed at 1250 K, finally, it was quickly quenched in the cold distilled water. After another drying, fine silica powder was obtained which was next used in sample preparation.

The appropriate amounts of silica and other oxides were mixed and pelletized into small, cylindrical pellets. These pellets were inserted into electrolyte tubes and placed on the top of the metal. After metal and oxides heating and melting such a liquid system was used as a working electrode of the cell. Solid electrolyte tubes CSZ closed at one end (length 400 mm, $\phi = 8$) and YSC (length 50 mm, $\phi = 6$) were supplied by Yamari Trading Co., Japan.

Technique

Two types of e.m.f. cells were used in our experiments and they are shown in Figures 1a and 1b, respectively. The cell construction differs depending on the investigated system and the type of the reference electrode used during measurements. The first cell (Fig.1a) was employed during e.m.f. measurements in Pb-PbO and Pb-(PbO+SiO₂) liquid system, while the other one, was used to measure e.m.f.'s produced by the Pb-(PbO+Sb₂O₃+SiO₂) working electrode (Fig.1b).

In the first cell (Fig.1a), the tube of solid zirconia electrolyte contained about 2 g of metallic lead and the pellet of PbO or PbO-SiO₂ oxide mixture of a chosen composition. Dry air which acts as a reference electrode flowed in the outer furnace compartment and was flushing the electrolyte tube from the outside. Platinum wire was used as a connection to the outer part of the electrolyte tube's bottom. The working electrode was flushed inside the electrolyte tube with purified argon. The leads from the liquid electrode of the cell were made of a piece of iridium wire electrically welded to Kanthal wire. The whole cell was put into a constant temperature zone of the vertical resistance furnace.

In the other cell (Fig. 1b) the reference electrode was a mixture of Ni+NiO powders in the molar ratio 1.5:1. The investigated electrode contained, at first, antimony and then lead together with the appropriate mixture of oxides.

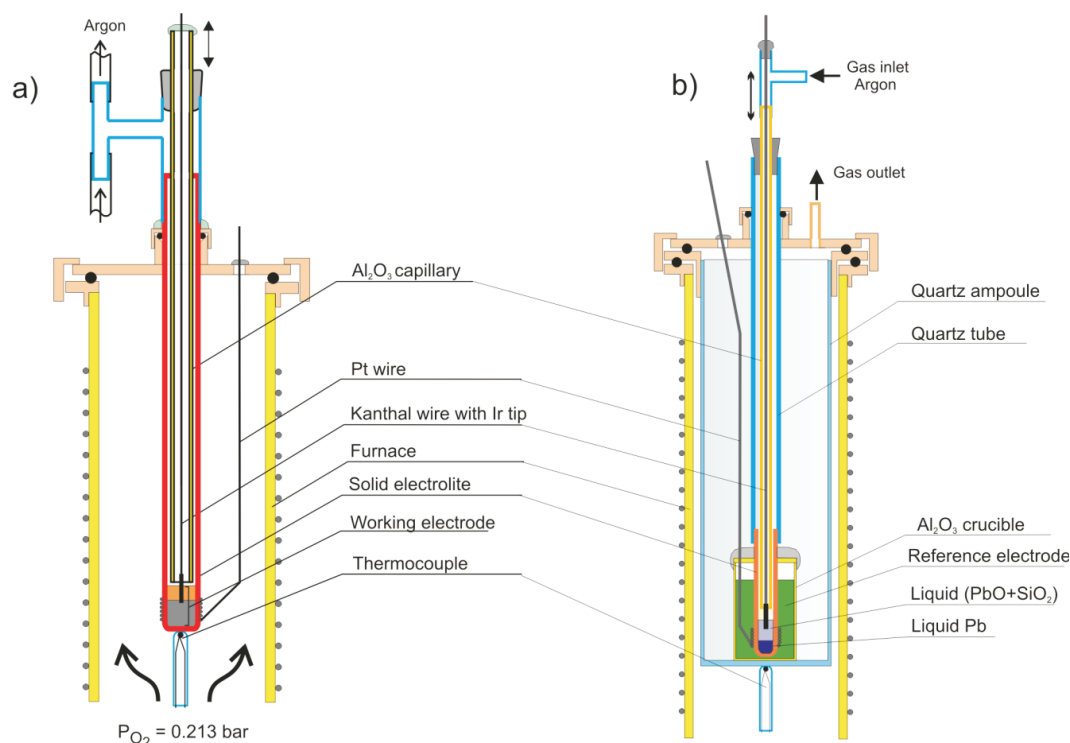


Fig. 1. The design of two types of e.m.f. cells: with air reference electrode ($P_{O_2} = 0.213$ bar) (a) and with Ni/NiO reference electrode (b)

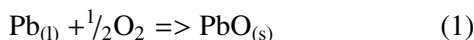
The working electrode and reference electrode were placed in a crucible made of alumina, sealed with high temperature cement and placed in a quartz tube closed at one end. Before experiments the whole system was flushed with pure argon.

Once the temperature was raised, it was controlled by Eurotherm controller, and e.m.f. was measured by high-resistance Keithley 2000 multimeter. The course of experiment (data necessary to reach equilibrium by the system) was controlled by check of e.m.f. vs. time curve slope acquired by a computer program. The cell was working for about one week and the measurements were taken at increasing and decreasing temperature.

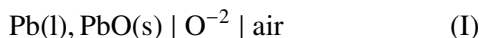
3. Results

3.1. Thermodynamic properties of PbO-SiO₂ liquid solutions

At the beginning Gibbs energy of formation of solid PbO according to the reaction:



was determined by the use of a galvanic cell:



in the temperature range 848-1123 K. It was calculated from the following formula:

$$\Delta G_{f,\text{PbO}}^0 = -2 \cdot F \cdot E^0 + 0.5 \cdot R \cdot T \ln P_{\text{O}_2}, \quad (2)$$

where: $P_{\text{O}_2} = 0.213$ bar denotes oxygen partial pressure at the air reference electrode, E^0 is an electromotive force of the cell (I), F is a Faraday constant. Finally, T and R are an absolute temperature and a gas constant, respectively.

Electromotive force values obtained in this work were corrected with thermo e.m.f. of (Kanthal+Ir)-Pt junction $\{E_{(\text{Kanthal+Ir})-\text{Pt}} (\text{mV}) = -0.2364 - 5.458 \cdot 10^{-4} \cdot T + 8.316 \cdot 10^{-6} \cdot T^2\}$.

Using corrected e.m.f. vs. T dependence in the form:

$$E(\text{V}) = 1.1181(\pm 0.0013) - 53.33 \cdot 10^{-5}(\pm 1.36 \cdot 10^{-6}) \cdot T \quad (3)$$

$\Delta G_{f,\text{PbO}}^0$ for the formation of the solid lead oxide was derived directly from equation (2) in the following form:

$$\Delta G_{f,\text{PbO}}^0 (\text{J} \cdot \text{mol}^{-1}) = -215771(\pm 260) + 96.43(\pm 0.3) \cdot T \quad (4)$$

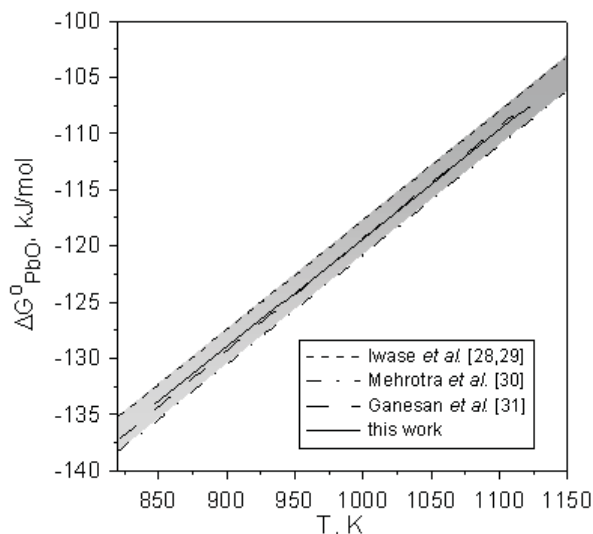
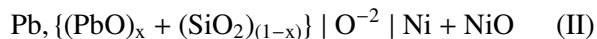


Fig. 2. The comparison of Gibbs energy of formation of solid β -PbO. All reviewed experimental data are bracketed by the lines representing results of Iwase *et al.* [28, 29] and Mehrotra *et al.* [30] shown as shadowed stripe. The newest results of $\Delta G_{f,\text{PbO}}^0$ of solid PbO [31] were superimposed

The results of Gibbs energy of formation of solid β -PbO (β -PbO, orthorhombic), $\Delta G_{f,\text{PbO}}^0$, as a function of temperature are compared in Fig. 2 with earlier experimental data reviewed by Risold *et al.* [27]. The line representing the obtained $\Delta G_{f,\text{PbO}}^0$ values is bracketed in the middle of the most extreme literature results [28, 29] and [30]. It means that all other 12 sets of data¹⁾ between them. Additionally, the newest results of Gibbs energy of formation of solid β -PbO [31] were superimposed (Fig. 2).

A good agreement is found between literature data and present results obtained for $\Delta G_{f,\text{PbO}}^0$ because the spread of data is about 2.5% of measured value and in case of comprehensive review of Ganesan *et al.* [31] is less than 0.5%. Consequently, one can believe that the determination of thermodynamic properties of oxide systems by the use of our experimental setup is accurate and reliable.

To determine PbO activity in the liquid slag the e.m.f. of the cell II:

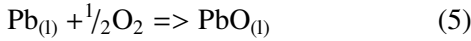


was measured in the temperature range from 1050 to 1300 K. The scheme of the cell is written in such a way that the right-hand electrode is a positive one.

In comparison with the cell I the reference electrode was changed (Fig. 1b) in order to reduce measured e.m.f. and to increase the precision of measurements.

The overall cell I reaction is:

¹⁾ The thermochemical calorie was adopted in present calculations: $1 \text{ cal}_{\text{th}} = 4.184 \text{ J}$



and for the reversible reaction (1) the change in Gibbs free energy can be expressed as follows:

$$\Delta G = -2F \cdot E = \mu_{\text{PbO}} - \mu_{\text{Pb}} - \frac{1}{2}\mu_{\text{O}_2} \quad (6)$$

while

$$RT \cdot \ln a_{\text{PbO}} = \Delta G_{\text{NiO}}^0 - \Delta G_{\text{PbO}}^0 - \Delta G_{\text{PbO}}^{s-1} - 2F \cdot E \quad (7)$$

Electromotive force values E obtained in this work by the use of cell (II) and corrected with thermo e.m.f. of (Kanthal+Ir)-Pt junction are shown in Fig. 3. The results of e.m.f. measurements were treated by least-squares analysis and obtained equations are given in Table 1.

Thermodynamic data of formation of liquid PbO in reaction (5) was calculated taking into account ΔG_{PbO}^0 expressed by equation (4) and the assessed by Risold *et al.* [27] Gibbs energy of fusion of pure, β -PbO (orthorhombic):

$$\Delta G_{\text{PbO}}^{\beta-1} (\text{J/mol}) = 26500 - 22.9 \cdot T \quad (8)$$

TABLE 1

The experimental e.m.f. vs. temperature for different composition of PbO-SiO₂ liquid solutions

X_{PbO}	e.m.f., $E(\text{V}) = A + B \cdot T$
0.8	$-0.2699 (\pm 0.0143) + 10.661 \cdot 10^{-5} (\pm 1.19 \cdot 10^{-3}) \cdot T$
0.7	$-0.2522 (\pm 0.0391) + 9.975 \cdot 10^{-5} (\pm 3.2 \cdot 10^{-3}) \cdot T$
0.667	$-0.2460 (\pm 0.0391) + 9.590 \cdot 10^{-5} (\pm 3.2 \cdot 10^{-3}) \cdot T$
0.6	$-0.2118 (\pm 0.00392) + 9.590 \cdot 10^{-5} (\pm 3.24 \cdot 10^{-6}) \cdot T$
0.5	$-0.2904 (\pm 0.00579) + 18.511 \cdot 10^{-5} (\pm 4.78 \cdot 10^{-6}) \cdot T$

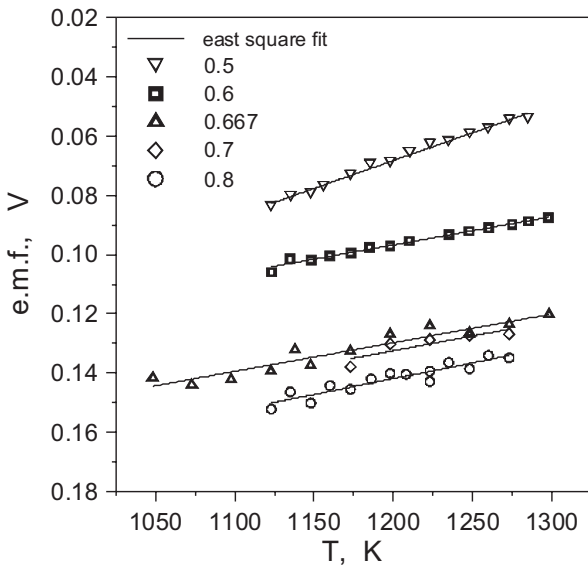


Fig. 3. Temperature dependence of e.m.f. of the cell II for different X_{PbO} concentration

The Gibbs energy of formation of solid NiO,

$\Delta G_{\text{f,NiO}}^0$ obtained from e.m.f. measurements by Kale and Fray [32] was accepted in PbO activity calculations with the use of equation 7. The activities of PbO in the liquid slag calculated directly from measured e.m.f.'s are shown in Fig. 4 as a function of PbO mole fraction at the chosen temperature 1273 K. These results indicate large negative deviation from the Raoult's Law, which in fact is compatible with the existence of solid silicates in this system.

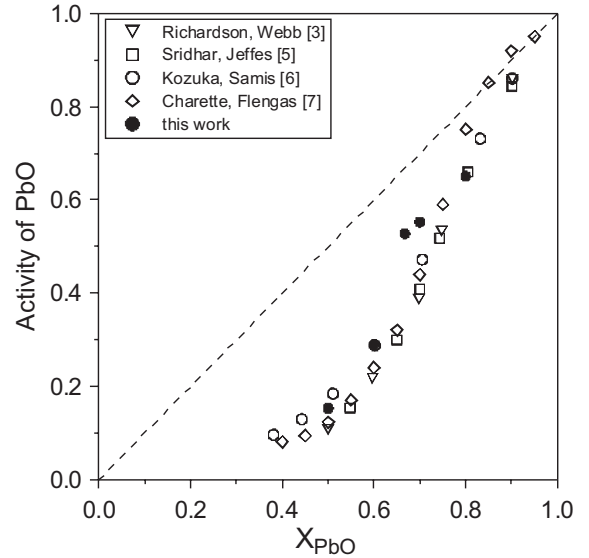
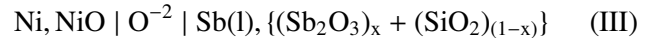


Fig. 4. The activity of PbO in PbO-SiO₂ liquid slag in the frame of experimental temperature range obtained at 1273 K

The PbO activity measurements together with the Østvold and Kleppa [9] enthalpies of solution data were used for the optimization of thermodynamic parameters of PbO-SiO₂ liquid slag by means of methods similar to [33, 34].

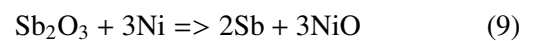
3.2. Thermodynamic properties of Sb₂O₃-SiO₂ liquid solutions

At first, the cell of the type:



was used to determine activity of Sb₂O₃ in the liquid phase. Since there is no information about the Sb₂O₃-SiO₂ phase diagram, it was assumed that because of substantial difference in melting points of pure component oxides, one may expect that the range of compositions available for experiments is located on Sb₂O₃-rich side. Two compositions $X_{\text{Sb}_2\text{O}_3} = 0.6$ and 0.7 were arbitrarily chosen for investigations.

The overall cell III reaction is:



and since for such a reaction the Gibbs free energy change is:

$$\Delta G = -6 \cdot F \cdot E = 2\mu_{\text{Sb}} + 3\mu_{\text{NiO}} - \mu_{\text{Sb}_2\text{O}_3} - 3\mu_{\text{Ni}} \quad (10)$$

it is easy to show that for pure, liquid Sb_2O_3 ($a_{\text{Sb}_2\text{O}_3} = 1$) standard Gibbs energy of formation of liquid antimony sesquioxide can be obtained from the measured e.m.f. of cell III, E^0 :

$$\Delta G_{\text{f},\text{Sb}_2\text{O}_3}^0 = -6F \cdot E^0 + 3\Delta G_{\text{f},\text{NiO}}^0 \quad (11)$$

The results of our measurements are shown in Figure 5 and 6, respectively and are gathered in Table 2. Gibbs free energy change of the reaction of formation of pure liquid antimony sesquioxide ($T_m = 929$ K) was calculated from equation (11) in the form:

$$\Delta G_{\text{f},\text{Sb}_2\text{O}_3}^0, \text{ J/mol} = -679376(\pm 780) + 233.17(\pm 0.77) \cdot T, \quad (12)$$

TABLE 2

Dependence of e.m.f. vs. temperature for particular composition of Sb_2O_3 - SiO_2 liquid solution

$X_{\text{Sb}_2\text{O}_3}$	e.m.f., E(V) = A + B · T
1	-0.04625 (± 0.001347) + 4.233 · 10 ⁻⁵ (± 1.34 · 10 ⁻⁶) · T
0.6	-0.03921 (± 0.01477) + 3.826 · 10 ⁻⁵ (± 1.19 · 10 ⁻⁵) · T
0.7	-0.03636 (± 0.00178) + 3.440 · 10 ⁻⁵ (± 1.74 · 10 ⁻⁶) · T

and shown in Fig. 5 together with the results of Sugimoto *et al.* [18] and Isecke [35], the most extreme literature results. It means that all other 8 sets of data [36-38] fall within the narrow shadowed area and additionally, most of the experimental data lies between the results of Sugimoto *et al.* [18] and the present data. The spread of the data is less than 2.2 % of the measured value. This excellent agreement between literature data and the present results of $\Delta G_{\text{f},\text{Sb}_2\text{O}_3}^0$ can be treated as a proof of reliability of galvanic cell III performance.

Next, the activity of Sb_2O_3 in the liquid solution $(\text{Sb}_2\text{O}_3)_x + (\text{SiO}_2)_{(1-x)}$ ($0 < x < 1$) can be obtained from the relation:

$$\ln a_{\text{Sb}_2\text{O}_3} = \frac{6F}{RT} \cdot (E^0 - E), \quad (13)$$

where measured E values are given in Table 2 in the form of A + BT equations.

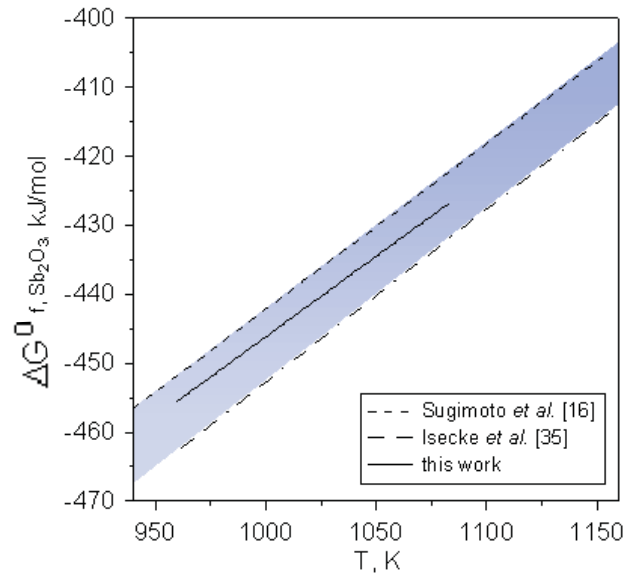


Fig. 5. The comparison of Gibbs energy of formation of liquid Sb_2O_3 with the literature data. All reviewed experimental data are bracketed by the lines representing results of Sugimoto *et al.* [18] and Isecke [35] shown as shadowed area

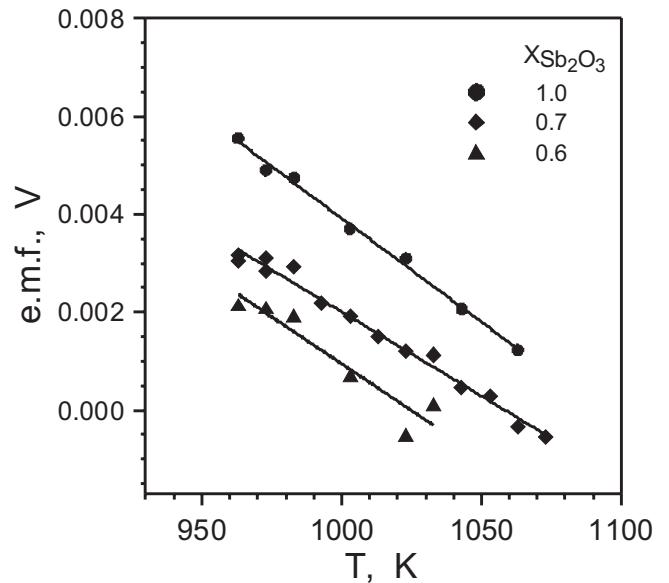


Fig. 6. Temperature dependence of e.m.f. of the cell III for pure liquid Sb_2O_3 and for different $X_{\text{Sb}_2\text{O}_3}$ concentrations of Sb_2O_3 - SiO_2 liquid solution

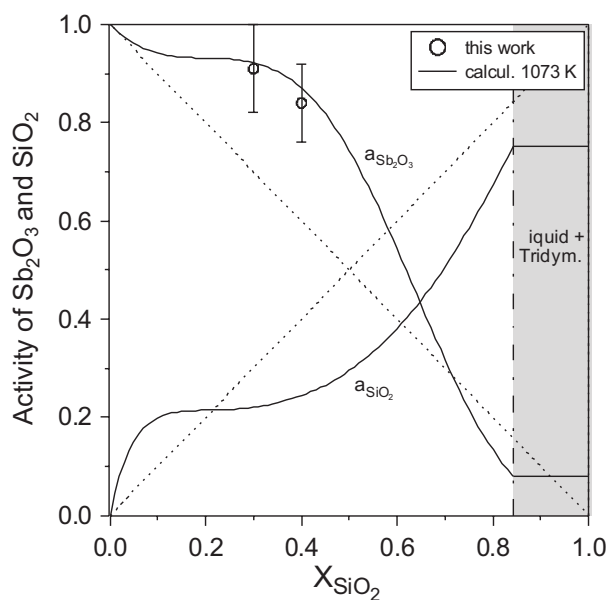


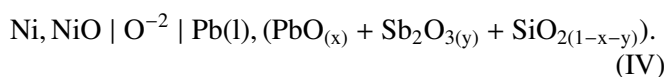
Fig. 7. The estimated activity of Sb_2O_3 and SiO_2 in Sb_2O_3 - SiO_2 liquid slag

It was found that the measured e.m.f.'s are very small and do not differ much from the result obtained for pure Sb_2O_3 . Calculated Sb_2O_3 activity values at 1073 K for $X_{\text{Sb}_2\text{O}_3} = 0.6$ and 0.7 are found to be 0.84 and 0.91, respectively. Considering experimental uncertainty this is in fact constant value. It may indicate that there exists a two phase field on Sb_2O_3 -rich side.

Activities are shown in Fig. 7 but taking into account very small values of measured e.m.f.'s the results are very uncertain. Therefore, another attempt was made to estimate the properties of the considered binary system.

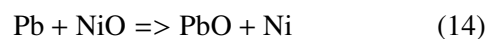
3.3. Thermodynamic properties of PbO - Sb_2O_3 - SiO_2 liquid solutions

Activity of PbO in the liquid PbO - Sb_2O_3 - SiO_2 ternary solution was measured using the cell of type IV:



Measurements were carried out along the cross-section of the ternary system with $X_{\text{PbO}}/X_{\text{SiO}_2} = 2$, and for the slag compositions $X_{\text{Sb}_2\text{O}_3} = 0.1, 0.2, 0.3$ and 0.4 . On the basis of the literature information about the thermodynamic properties of PbO - SiO_2 and PbO - Sb_2O_3 liquid solutions it was hoped that from the results obtained for the ternary system the interaction parameters characteristic of the binary Sb_2O_3 - SiO_2 solution may be derived.

The net cell IV reaction can be expressed in the form:



which is analogous to net reaction of cell II. So, the calculation of the activity of liquid PbO in the slag phase follows the previously described procedure and is described by the expression (7) where E is measured e.m.f. of cell IV.

TABLE 3
Dependence of e.m.f. vs. temperature for particular concentration of PbO - SiO_2 - Sb_2O_3 liquid slag

$X_{\text{Sb}_2\text{O}_3}$	e.m.f., $E(\text{V}) = A + B \cdot T$
0.1	$-0.19627 (\pm 0.0112) + 8.900 \cdot 10^{-5} (\pm 9.58 \cdot 10^{-6}) \cdot T$
0.2	$-0.13967 (\pm 0.0143) + 5.557 \cdot 10^{-5} (\pm 1.21 \cdot 10^{-5}) \cdot T$
0.3	$-0.14848 (\pm 0.0092) + 7.006 \cdot 10^{-5} (\pm 7.95 \cdot 10^{-6}) \cdot T$
0.4	$-0.16643 (\pm 0.0123) + 9.9304 \cdot 10^{-5} (1.05 \pm 10^{-5}) \cdot T$

The results produced by cell IV are shown in Fig. 8 and are also gathered in Table 3. In our case experiments for higher Sb_2O_3 concentrations were not possible since for the sample of $X_{\text{Sb}_2\text{O}_3} = 0.4$ microprobe detected antimony in the lead used in the working electrode of cell IV. This speaks for the side reaction between the slag phase and the metal for higher Sb_2O_3 content, which makes experiments for higher Sb_2O_3 concentrations impossible.

The calculated PbO activities for the ratio $\text{PbO}/\text{SiO}_2 = 2$ are shown in Fig. 9 as a function of $X_{\text{Sb}_2\text{O}_3}$ at 973 and 1173 K, respectively. In the same Figure activities of Sb_2O_3 determined at 973 K by McClincy and Larson [20] from vapor pressure measurements are also shown. Despite different techniques both sets of the data agree reasonably well.

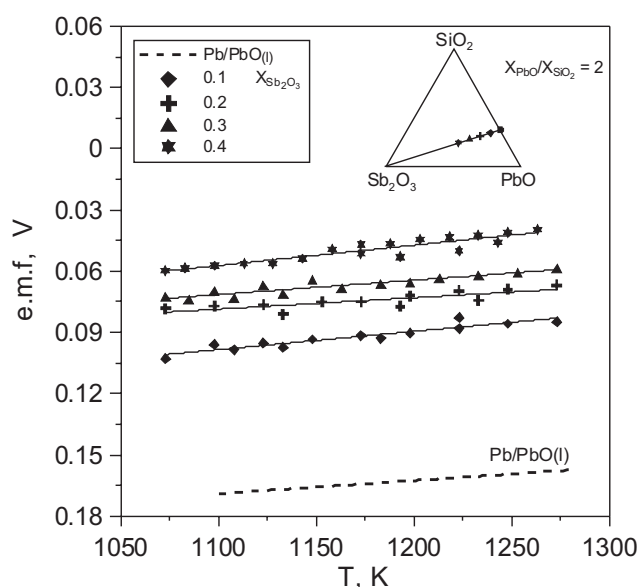


Fig. 8. Temperature dependence of e.m.f. of the cell IV for different X_{PbO} concentration

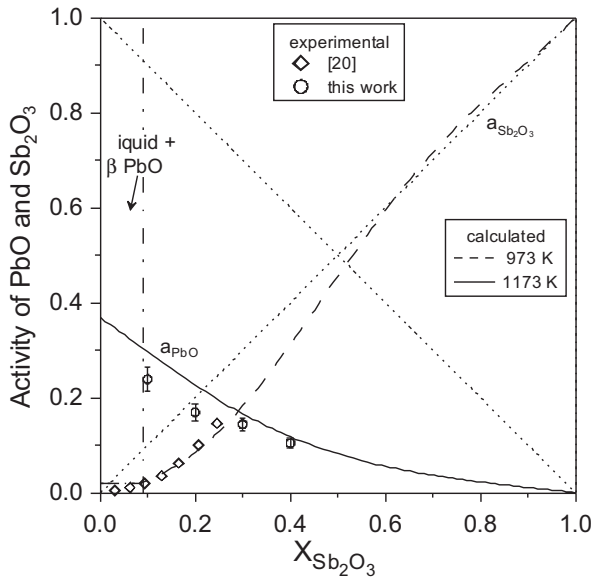


Fig. 9. The comparison of calculated and measured activity of Sb_2O_3 [20] and PbO in $\text{PbO-Sb}_2\text{O}_3\text{-SiO}_2$ liquid slag for $\text{PbO/SiO}_2 = 2$ at 973 K and 1173 K, respectively

4. Thermodynamic assessment and phase diagrams estimation

A quasi-regular solution model was applied to describe the binary liquid phase. The molar Gibbs energy of solution phase is expressed by the equation:

$$G_m = x_A^0 G_A + x_B^0 G_B + RT(x_A \cdot \ln x_A + x_B \cdot \ln x_B) + {}^{\text{ex}} G_m \quad (15)$$

The parameter ${}^0 G_i$ is the Gibbs energy of pure oxide species i , i.e. PbO , Sb_2O_3 and SiO_2 . Their values were taken from [27], [39] and [40], respectively,

The excess free energy is expressed as quasi-regular solution [44] by formula:

$${}^{\text{ex}} G_m = x_A x_B \cdot \sum_{i=0} (x_A - x_B)^i \cdot {}^i L_{A,B}, \quad (16)$$

where ${}^i L_{A,B}$ interaction parameters are temperature dependent and given in $\text{J}\cdot\text{mole}^{-1}$. When thermodynamic data for terminal solutions are not available an assumption was made that the mutual solid solubility of SiO_2 , PbO or/and Sb_2O_3 is negligible.

The thermodynamic evaluation was carried out by the optimization and calculation program, TCCR (ThermoCalc AB Stockholm) [42] and Pandat 7.0, developed by Computherm LLC (USA) [43]. Using the obtained activity values, the thermodynamic properties of the liquid solutions were described with Redlich-Kister formula (16).

4.1. $\text{PbO}+\text{SiO}_2$ system

$\text{PbO}+\text{SiO}_2$ system was modeled using the obtained activity values and the data published in the literature [3, 5-7], the liquidus data [45-50] and the enthalpies of solution of liquid lead oxide in PbO-SiO_2 melts at 1173 K [9]. The parameters of excess Gibbs free energy according to the formalism (16) were collected in Table 4. The comparison between calculated and experimentally obtained thermodynamic data are shown in Fig. 10 and 11.

From this equation all thermodynamic functions for the liquid solutions can be determined. Parameters ${}^i L_{\text{PbO,SiO}_2}$ are linearly dependent on temperature and are given in $\text{J}\cdot\text{mole}^{-1}$.

The Gibbs energy of the stoichiometric phases was given relatively to the Gibbs energy of pure oxide species ${}^0 G_i$ by the equation:

$$G_{(p,q)} = p^0 G_A + q^0 G_B + \Delta^0 G_{f,(p,q)}, \quad (17)$$

where $\Delta^0 G_{f,(p,q)}$ is a Gibbs energy of formation of A_pB_q compound and p, q are the stoichiometric coefficients. $\Delta^0 G_{f,(p,q)}$ can be expressed as a sum of enthalpy and entropy terms in ($\text{J}\cdot\text{mole}^{-1}$):

$$\Delta^0 G_{f,(p,q)} = \Delta^0 H_{(p,q)} - T \cdot \Delta^0 S_{9(p,q)} \quad (18)$$

TABLE 4
Optimized model parameters of the PbO-SiO_2 phases

Parameter	Value and linear dependence on temperature, $\text{J}\cdot\text{mole}^{-1}$
Liquid phase	Substitutional model
${}^0 L_{\text{PbO,SiO}_2}$	$-33605.1 + 2.3701 \cdot T$
${}^1 L_{\text{PbO,SiO}_2}$	$-13551.2 - 7.7051 \cdot T$
${}^2 L_{\text{PbO,SiO}_2}$	$19293.2 - 2.4049 \cdot T$
Phase Pb_4SiO_6	Linear compound
$\Delta^0 G_{f,\text{Pb}_4\text{SiO}_6}$	$-28837 - 5.5883 \cdot T$
Phase Pb_2SiO_4	Linear compound
$\Delta^0 G_{f,\text{Pb}_2\text{SiO}_4}$	$-29859 - 1.7761 \cdot T$
Phase PbSiO_3	Linear compound
$\Delta^0 G_{f,\text{PbSiO}_3}$	$-16850 - 5.0982 \cdot T$

Using this thermodynamic description of the liquid phase, Gibbs free energy of formation of both silicates, and available data on phase equilibria, the binary $\text{PbO}+\text{SiO}_2$ system was calculated and is shown in Fig. 12.

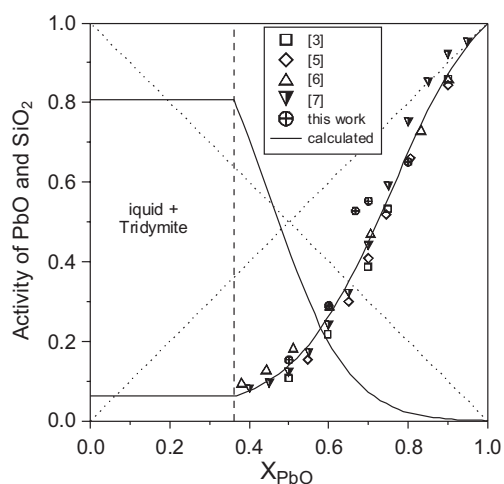


Fig. 10. The activity of PbO and SiO₂ in PbO-SiO₂ liquid slag calculated at 1273 K. The experimental data [3, 5-7] are superimposed

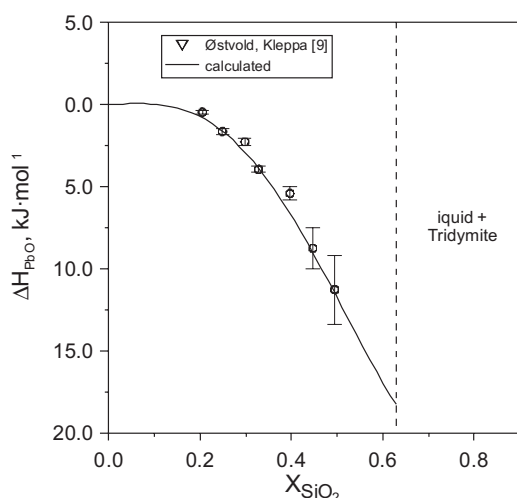


Fig. 11. Optimized partial enthalpies of solution of liquid lead oxide in PbO-SiO₂ melts at 1173 K

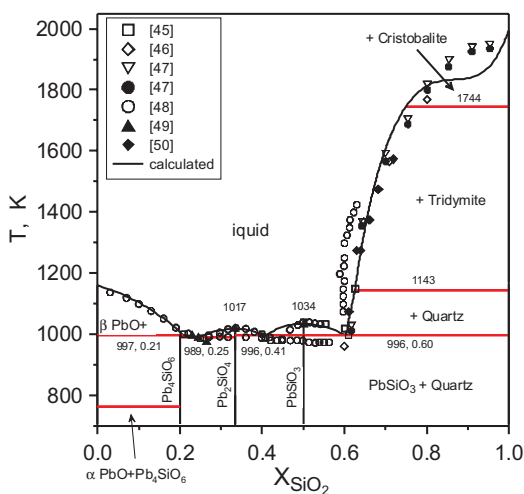


Fig. 12. Optimized PbO-SiO₂ phase diagram. Experimental data [45-50] are superimposed

The assessment of PbO-SiO₂ system published by Jak *et al.* [51], despite a good thermodynamic model-

ing, was not adopted in the present analysis because the associate solution model used in it for liquid solution is too complicated for our estimation of the activity in the PbO-Sb₂O₃-SiO₂ system.

4.2. PbO+Sb₂O₃ system

The description of the thermodynamic properties of another binary system, namely PbO-Sb₂O₃, is based on the phase diagram experimental data found in literature [13,16-18] and the data of Sb₂O₃ activity in the liquid oxide phase at temperatures range 973-1223 K [13, 18-20]. The obtained excess Gibbs free energy parameters used in our calculations are gathered in Table 5.

The compound PbSb₂O₄ presented in Fig. 13 is tentative but still it is hard to agree that its congruent melting temperature (1653 K) reported in [52] is realistic. The interpretation of the onset temperature in DTA measurements is a well known problem, especially, in viscous slag forming systems. In this case the experimental error can be substantial.

Consequently, for the equimolar compound PbSb₂O₄, melting temperature at 843 K [53] is probably close to reality.

TABLE 5

Optimized model parameters of the PbO-Sb₂O₃ phases

Parameter	Value and linear dependence on temperature, J·mole ⁻¹
Liquid	Substitutional model
⁰ L _{PbO,Sb₂O₃}	-63759.3 + 35.0117 · T
¹ L _{PbO,Sb₂O₃}	-579.6
Phase PbSb ₂ O ₄	Linear compound
Δ ⁰ G _{f,PbSb₂O₄}	-107079 + 103.3 · T

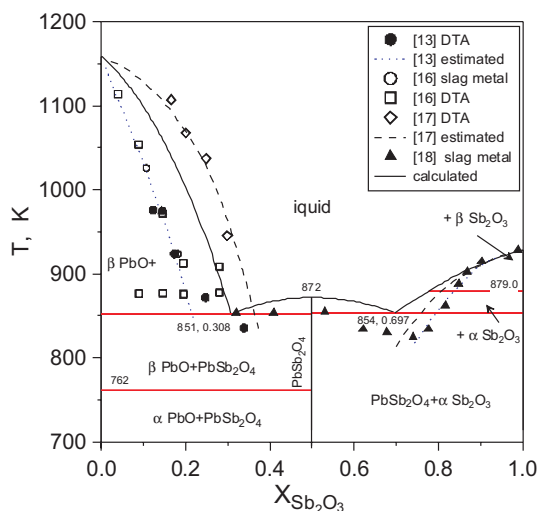


Fig. 13. Optimized PbO-Sb₂O₃ phase diagram. Experimental data [13, 16-18] were superimposed

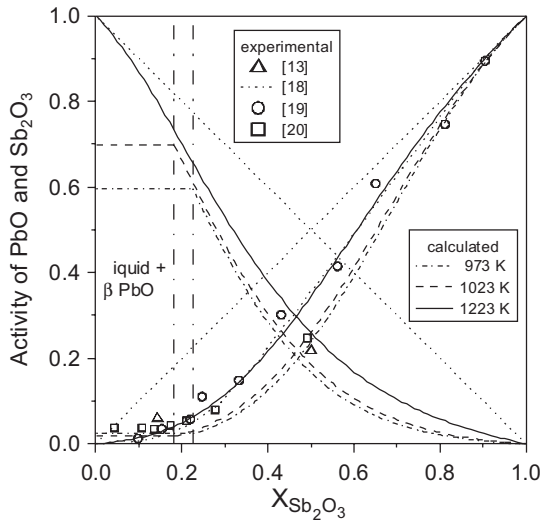


Fig. 14. The activity of PbO and Sb_2O_3 in $\text{PbO-Sb}_2\text{O}_3$ liquid slag calculated at 973 K, 1023 K and 1223 K. The experimental data [13, 18-20] were superimposed

4.3. $\text{Sb}_2\text{O}_3+\text{SiO}_2$ and $\text{PbO-Sb}_2\text{O}_3\text{-SiO}_2$ systems

In the case of $\text{Sb}_2\text{O}_3+\text{SiO}_2$ system the adopted procedure of calculations was slightly different. Having the activity of lead and antimony oxides determined along the vertical cross-section of the $\text{PbO-Sb}_2\text{O}_3\text{-SiO}_2$ system, and the activity of Sb_2O_3 in the binary system, one can use Redlich-Kister-Muggianu model [41, 54] to derive interaction parameters for binary $\text{Sb}_2\text{O}_3\text{-SiO}_2$ liquid solution. Because there is no thermodynamic information about this system, the term describing ternary interactions were not taken into account. The obtained model parameters are gathered in Table 6. Calculated activities in the binary system are shown in Fig. 7 and compared at 1073 K with measured our values.

Using the obtained model parameters the phase diagram for $\text{Sb}_2\text{O}_3+\text{SiO}_2$ system was predicted and is shown in Fig. 15. It indicates the existence of a small miscibility gap. This is contrary to PbO-SiO_2 and $\text{Bi}_2\text{O}_3+\text{SiO}_2$ systems, where solid silicate phases are present, and the liquid solutions exhibit negative deviations from the Raoult's Law. Finally, the model calculations were extended upon the ternary system. Activities of Sb_2O_3 determined at 973 K from vapor pressure measurements by McClincy and Larson [20] are shown and compared with the results of calculations in Fig. 9. Also, a_{PbO} obtained from our e.m.f. measurements are shown in the same Figure. Considering the uncertainty in the description of binary systems the overall agreement is good. The predicted liquidus in the ternary $\text{PbO-Sb}_2\text{O}_3\text{-SiO}_2$ system is shown in Fig. 16. Respective invariant reactions for both unknown binary and ternary systems are gathered in Table 7.

TABLE 6

Optimized model parameters of the $\text{Sb}_2\text{O}_3\text{-SiO}_2$ phases

Parameter	Value, $\text{J}\cdot\text{mole}^{-1}$
Liquid	Substitutional model
${}^0\text{L}_{\text{Sb}_2\text{O}_3\text{SiO}_2}$	-2314.8
${}^1\text{L}_{\text{Sb}_2\text{O}_3\text{SiO}_2}$	16483.6

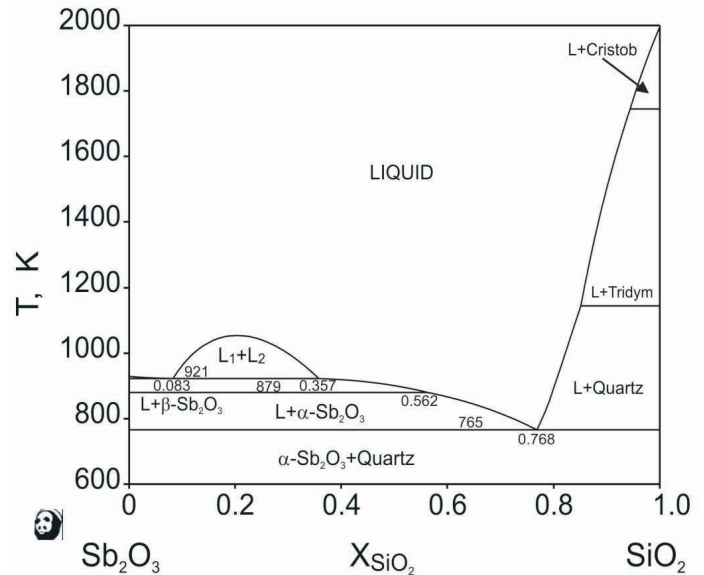


Fig. 15. Estimated $\text{Sb}_2\text{O}_3\text{-SiO}_2$ system

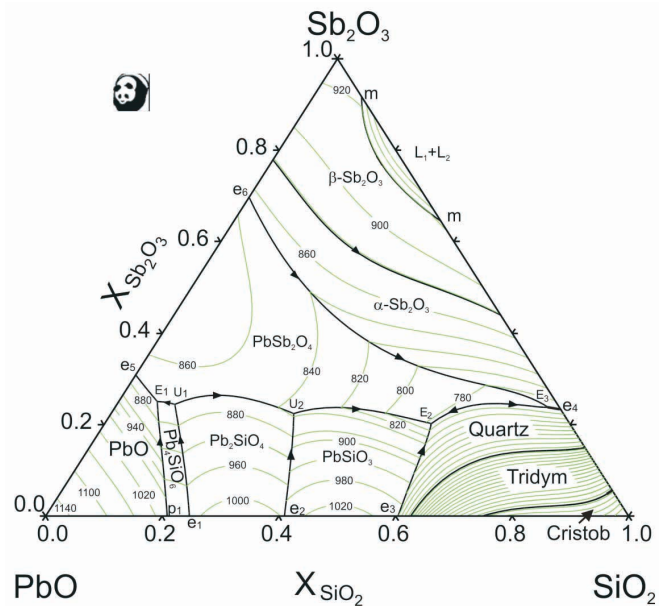


Fig. 16. Estimated liquidus in pseudoternary $\text{PbO-Sb}_2\text{O}_3\text{-SiO}_2$ system

TABLE 7

Binary and ternary invariant reactions in PbO-Sb₂O₃-SiO₂ pseudoternary system

Invariant Reaction		T, K	X _{PbO}	X _{Sb₂O₃}	X _{SiO₂}
U1	Liquid + Pb ₂ SiO ₄ → PbSb ₂ O ₄ + Pb ₄ SiO ₆	845.7	0.6569	0.2437	0.0994
E1	Liquid → PbSb ₂ O ₄ + Pb ₄ SiO ₆ + β-PbO	844.1	0.6839	0.2499	0.0662
U2	Liquid + Pb ₂ SiO ₄ → PbSb ₂ O ₄ + PbSiO ₃	833.7	0.4632	0.2236	0.3132
E2	Liquid → Quartz + PbSb ₂ O ₄ + PbSiO ₃	777.5	0.2382	0.2016	0.5602
E3	Liquid → α-Sb ₂ O ₃ + Quartz + PbSb ₂ O ₄	761.0	0.0204	0.2372	0.7424
e1	Liquid → Pb ₄ SiO ₆ + Pb ₂ SiO ₄	989	0.75	–	0.25
e2	Liquid → Pb ₂ SiO ₄ + PbSiO ₃	996	0.59	–	0.41
e3	Liquid → PbSiO ₃ + Quartz	996	0.4	–	0.60
e4	Liquid → α-Sb ₂ O ₃ + Quartz	765	–	0.232	0.768
e5	Liquid → β-PbO + PbSb ₂ O ₄	851	0.692	0.308	–
e6	Liquid → α-Sb ₂ O ₃ + PbSb ₂ O ₄	854	0.303	0.697	–
p1	Liquid + β-PbO → Pb ₄ SiO ₆	997	0.79	–	0.21
m	Liquid ₁ → Liquid ₂ + α-Sb ₂ O ₃	921	–	0.917	0.083

5. Conclusions

In this study the predicted ternary PbO-Sb₂O₃-SiO₂ oxide phase diagram has been suggested. Attempts have also been made to determine the thermodynamic properties of the liquid phase in Sb₂O₃-SiO₂ system as well as to calculate this pseudobinary phase diagram. Though the predicted diagrams are probably not exact they may be not far from reality for the following reasons:

- Gibbs free energy of formation of pure oxides PbO and Sb₂O₃ determined from our e.m.f. measurements is in good agreement with the data taken from literature. This speaks for the precision of our measurements and reversible cell operation.
- Thermodynamic properties of the liquid PbO-SiO₂ solutions represented by measured activities are also in reasonable agreement with the literature data. This fact demonstrates that the side reactions in the cell due to aggressive liquid phase were under control.
- Using available thermochemical and phase diagram data calculations of two binary oxide systems, namely PbO-SiO₂ and PbO-Sb₂O₃ were carried out and good agreement was found between the calculated and experimentally determined phase diagrams. Calculations were performed under the assumption that there are no associates in binary melts. Because of the lack of sufficient data the ternary interaction in the liquid slag was omitted.
- CALPHAD method proved to be successful in predicting unknown phase diagrams with the aid of minimal amount of the experimental data. The thermodynamic description of Sb₂O₃-SiO₂ system is tentative but coherent. Attempts to estimate the temperature dependence of liquid phase parameters were not successful.
- Finally, gathered parameters for the liquid phase

existing in respective binary systems are the foundation of the database built with the purpose of describing the thermodynamic properties of Kaldo process slags. This work should be continued for other oxide systems.

REFERENCES

- [1] Phase Diagrams for Ceramists: 1975 supplement. Ed. E.M. Levin, H.F. Mc Murdie, The American Ceramic Society 1975, p. 4352.
- [2] R. J. Callow, Trans. Faraday Soc. **37**, 370 (1951).
- [3] F. D. Richardson, L. D. Webb, Trans. Ins. Min. Metall. **64**, 529 (1955).
- [4] V. I. Minenko, N. S. Ivanova, Ukr. Khim. Zhur. **29**, 1160-1164 (1963).
- [5] R. Sridhar, J. H. E. Jeffes, Trans. Ins. Min. Metall. C, **76**, 44-50 (1967).
- [6] Z. Kozuka, C. S. Samis, Met. Trans. **1**, 871-876 (1970).
- [7] G. G. Charette, S. N. Flengas, Canadian Met. Quart. **7**, 191-200 (1968).
- [8] M. L. Kapoor, M. G. Froberg, Archiv. Eisenhutte. **42**, 1 (1971).
- [9] T. Østvold, O. J. Kleppa, Inorg. Chem. **8**(1), 78-82 (1969).
- [10] J. C. Boivin, G. Tridot, C. R. Acad. Sc. Paris **278 C**, 865 (1974).
- [11] R. M. Biefeld, S. S. White, J. Amer. Ceram. Soc. **64**, 182 (1981).
- [12] G. M. Mehrotra, M. G. Froberg, M. L. Kapoor, Z. Metall. **67**, 186 (1976).
- [13] C. G. Maier, W. B. Hincke, AIME Tech. Pub. **449**, 3-12 (1932).
- [14] J. Barthel, Bergakademie **9**, 630 (1957).
- [15] E. Pelzel, Erzmetall **12**(11), 558-561 (1958).
- [16] A. D. Zunkel, A. H. Larson, Trans. Metal. Soc. AIME **239**, 473-477 (1967).

- [17] H. Hennig, E. J. Kohlmeier, *Erzmetall.* **10**, 8-15 (1957).
- [18] E. Sugimoto, S. Kuwata, Z. Kozuka, *J.Min. Metall.Inst.Japan* **98**, 429-435 (1982).
- [19] S. Itoh, K. Yamanishi, A. Kikuchi, *J.Min.Mater.Process.Inst. Japan* **117**, 138-142 (2001).
- [20] R. J. McClincy, A. H. Larson, *Trans. Metal. Soc. AIME* **245**, 23 (1969).
- [21] A. Tairi, J. C. Chmparnaud-Mesjard, D. Mercurio, B. Frit, *Rev. Chim. Min.* **22**, 699 (1985).
- [22] O. Turkoglu, M. Soylak, N. Kulcu, *Kuwait J. Sci. Eng.* **26**, 289 (1999).
- [23] L. Jingkui, Z. Yuling, F. Xing, *Chinese J. Low Temp. Phys.* **14**, 161 (1992).
- [24] V. B. Tshernogorenko, I. G. Donets, A. A. Semenov-Kobzar, I. V. Kursenko, L. V. Doncheva, *Ukr. Khim. Zhur.* **43**, 1058 (1977).
- [25] A. Krzyżak, K. Fitzner, *Met. Foundry Eng.* **29**, 81-95 (2003).
- [26] M. Kopyto, W. Przybyło, B. Onderka, K. Fitzner, (in preparation).
- [27] D. Risold, J.-I. Nagata, R. O. Suzuki, *J.Phase Equil.* **19**(3), 213-233 (1998).
- [28] M. Iwase, K. Fujimura, T. Mori, *J.Jpn.Inst.Met.* **39**, 1118-1127 (1975).
- [29] M. Iwase, K. Fujimura, T. Mori, *Trans.JIM* **19**, 377-384 (1975).
- [30] G. M. Mehrotra, PhD thesis, (1975), cited from Risold *et al.* [27].
- [31] R. Ganesan, T. Gnanasekaran, R. S. Srinivasa, *J.Nuclear Mater.* **320**, 258-264 (2003).
- [32] G. M. Kale, D. J. Fray, *Metall.Mater.Trans. B*, **25B**(6), 373 (1994).
- [33] J-R. Soh, H. M. Lee, H-S. Kwon, *Calphad* **18**(3), 237-244 (1994).
- [34] O. Beneš, R. J. M. Konings, *J.Alloys Comp.* **452**(1), 110-113 (2008).
- [35] B. Isecke, PhD thesis, Technical University Berlin, 1977.
- [36] B. Onderka, K. Fitzner, **86**(5), 313-318 (1995).
- [37] N. Kenmori, W. T. Denholm, S. Saunders, *Canadian Met. Quart.* **35**(3), 269-274 (1996).
- [38] A. Krzyżak, K. Fitzner, *Thermochim.Acta* **414**, 115-120 (2004).
- [39] SGTE Substance Database: SSUB3, http://www.thermocalc.com/Filer/Pdf/Manuals/TC_Database_Guide.pdf
- [40] O. Fabrichnaya, H. J. Seifert, R. Weiland, T. Ludwig, F. Aldinger, A. Navrotsky, *Z. Metallkd.* **92**(9), 1083-1097 (2001).
- [41] M. Hillert, *Phase Equilibria, Phase Diagrams and Phase Transformations: Their Thermodynamic Basis*, United Kingdom, Cambridge University Press, 2007.
- [42] B. Sundman, B. Jansson, J.-O. Andersson, *Calphad* **9**, 153-190 (1985).
- [43] Y. A. Chang, R. Schmid-Fetzer, W. A. Oates, *J. Mater.* **12**, 48-51 (2003).
- [44] O. Redlich, A. T. Kister, *Ind. Eng. Chem. Res.* **40**(2), 345-349 (1948).
- [45] R. F. Geller, A. S. Creamer, E. N. Bunting, *Res.Papier No.RP705*, NBS, Geithersburg, MD, Aug. 1934, pp. 237-244.
- [46] K. A. Krakau, E. J. Mukhin, M. S. Heinrich, *Dokl.Akad.Nauk SSSR* **14**, 281 (1937).
- [47] P. D. Calvert, R. R. Shaw, *J.Am.Ceram.Soc.* **53**(6), 374-375 (1970).
- [48] U. Kuxman, P. Fischer, *Erzmetall.* **27**(11), 533-537 (1974).
- [49] R. M. Smart, F. P. Glasser, *J.Am.Ceram.Soc.* **57**(9), 378-382 (1974).
- [50] E. Jak, B. Zhao, N. Liu, P. C. Hayes, *Metal. Mater.Trans. B*, **30B**, 21-27 (1999).
- [51] E. Jak, S. Degterov, P. Wu, P. C. Hayes, A. D. Pelton, *Metal.Mater.Trans. B*, **28B**, 1011-1018 (1997).
- [52] P. M. Milyan, O. O. Semrad, S. V. Kun, *Nauk. Visnyk UzhNU, Ser. Khim.* **6**, 138-143 (2001).
- [53] Webpage: Khimik, Database of thermodynamic properties of compounds: <http://www.xumuk.ru/tdsv/2830.html>
- [54] M. Muggianu, M. Gambino, J-P. Bros, *J.Chim.Phys.* **72**(1), 83 (1975).